A centrifuge – experimental study in the soil and structure interaction effect on a SDOF system

D. Taeseri, P. Martakis & E. Chatzi
ETH Zurich, Zurich, Switzerland

J. Laue
Lulea University of Technology, Lulea, Sweden

ABSTRACT: Soil Structure Interaction (SSI) refers to structural elements in contact with soil and implies the response of the system to an external loading. Up to now, the importance of this effect is not thoroughly taken into account in the design codes. In praxis, geotechnical engineers tend to replace the foundation with a stiff inclusion while structural engineers assume springs or fixed boundary conditions in simulating foundations. In this work, a set of centrifuge experiments are conducted in order to highlight the influence of specific soil and structural parameters within the context of the SSI effect. The chosen model represents a SDOF system founded on homogenous soil. The main purpose of this experimental and analytical work is to examine the influence of the slenderness ratio between structure and soil to the magnitude of the SSI effects. These effects are quantified through the commonly adopted index of Period Lengthening Ratio (PLR).

1 INTRODUCTION

The construction of a building starts at the foundation upon which the whole superstructure is built. For an adequate representation of the structural behavior, both in ultimate and service limit state, it is necessary to take the mutual dependence of soil and structure into account. Unfortunately, in most real-life construction projects, these effects are neglected. The craving for simple design calculations and the extensive specialization in the respective fields of geotechnical and structural engineering have led to a state where the only interface between structure and soil seems to be a matter of load and strength in rigid boundary conditions (Anastasopoulos et al. 2013). This is believed to be an assumption on the safe side, but this judgment is difficult in a case of seismic activities. Generally, the soil provides a more flexible dynamic behavior and also an increase in damping. The dynamic SSI under seismic events consists mainly of two phenomena. The kinematic interaction describes the motion of the soil and its action on the opposing foundation. On the other hand, the inertial interaction is caused by the transmission of the inertial force of the structure to the soil which leads to further deformations.

Goal of the study is to quantify the effect of soil-structure interaction (SSI) on the period lengthening ratio (PLR = T/T_1 or f_1/f), which is defined as the ratio of the natural period of the soil structure system (T or 1/f) to the first natural period of the fixed-base structure (T_1 or $1/f_1$).

In order to analyze the effect of SSI on the natural period, a set of structures as illustrated in Figure 1 is chosen. The equivalent structural model without soil interaction is fixed at its base. For the fixed-base structure a simple but reasonable structural model would be a cantilever with a mass on top. Therefore, the equivalent fixed-base structure comprises only one degree of freedom (1-DOF) and it is trivial to calculate its period T_1. Furthermore, to quantify the PLR, the natural period of the soil-structure system (T) is assessed by taking into account the soil parameters. A large set of different soil-structure configurations is examined to study the influence of fixed-base period T_1, foundation dimensions and soil stiffness parameters on the PLR (Sieffert & Cevaer 1995).

To reach this goal firstly, an analytical simplified model of the problem is suggested by modeling the soil with springs (Kausel et al. 1978). Secondly, experiments with models of the different structures are conducted in the geotechnical centrifuge and the structures vibration period is determined using system identification methods. Additionally, shear wave velocity of the sand in flight is determined from Spectral Analysis of Surface Waves (SASW) method (Nazarian & Stokoe 1984) in order to back-calculate its shear modulus at small strains. This

shear modulus is then used to update the stiffness of the springs in the analytical model. To conclude, the results of the centrifuge experiments and analytical solution are compared and discussed.

2 METHODS

The general purpose of the project is to understand the SSI effect on the response signal of the structure due to an impulse excitation. To be able to achieve this goal two different approaches were applied. Firstly, a simplified analytical solution was proposed based on previous research studies. Secondly, physical modeling experiments were conducted with the geotechnical drum centrifuge of the ETH-Zurich (Springman et al. 2001).

In total 14 different structures with various combinations of the superstructure height H, foundation width 2B and depth of embedment D were analyzed. Figure 1 summarizes schematically the variations studied. All dimension are in model scale and the centrifuge tests were conducted at 60g. The material of the foundation and the superstructure's column were in aluminum (E_{al} = 70 GPa & ρ_{al} = 2700 kg/m^3) and by contrast the head of the cylindrical superstructure was in steel.

The foundation is embedded in the so-called Perth sand, a rounded, poorly graded sand (D_{50} = 0.22 mm). Density properties are given in Table 1 (Peñuela 2013). The dry densities reached in these set of experiments were around 1700 kg/m^3.

Table 1. Perth sand densities and void ratio.

Specific density	Dry density	Void ratio
ρ_s	$\rho_{d,min}$ … $\rho_{d,max}$	e_{min} … e_{max}
2650 kg/m^3	1513 … 1765 kg/m^3	0.502 … 0.752

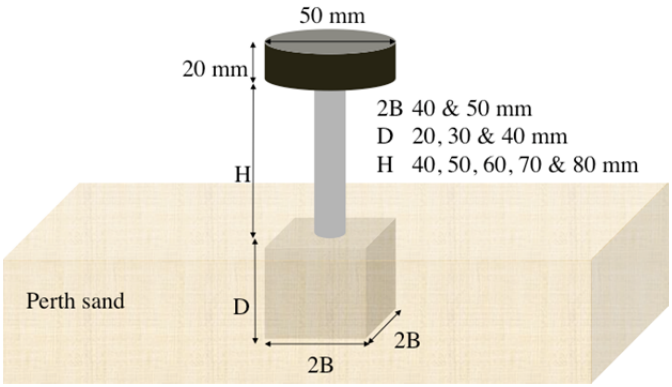

Figure 1. Schematic representation of the analyzed problem.

2.1 *Analytical method*

A simplified analytical model was developed to understand the dynamic response of the structure and to be able to analyze the influence of the different parameters on the natural frequency response of the soil-structure system. Additionally, the analytically determined natural frequency of the models can be compared to the experimentally identified frequency.

The analytical solution is based on simple mechanical and kinematic relations. Since the excitation has mostly an effect in one direction, the three-dimensional cantilever structure is simplified to a planar problem, shown in Figure 2.

The analytical approach to the problem is subdivided in four steps:

- Suggest an appropriate spring system model, which represents in the best possible way the SSI during an impulse excitation
- Calculate the analytical solution of the simplified model (equation of motion)
- Determine the stiffness of the springs as a function of the soil parameters
- Estimate the natural frequency of the soil-structure system.

2.1.1 *Spring model system*

The spring model system should reproduce the period of the first mode of the structure (rocking mode) accurately. For simplicity, all influences without appreciable effect on the first mode period are omitted. It is assumed that damping is small and therefore, the effect of damping on the first mode period is negligible.

The simplified spring model is illustrated in Figure 2a. Starting point for the simplification is the equivalent fixed base model of a cantilever with superstructure stiffness k_s and point mass m_1 on top. Additionally, the stiffness of the soil is modeled with two springs: one in rotational direction for modeling the resistance against rotation and the other one in horizontal direction for the resistance against horizontal displacement. The center of rotation is assumed to be on the level of the depth of embedment.

A triangular distribution of earth pressure is assumed and therefore the horizontal spring is located 1/3 D above the embedment depth. As only movements in horizontal direction are of interest, vertical movement is constrained. A second point mass m_2 is placed on bottom to take into account the weight of the foundation.

2.1.2 *Equation of motion*

In order to derive the equations of motion, the spring model is divided into two parts as illustrated in Figure 2b.

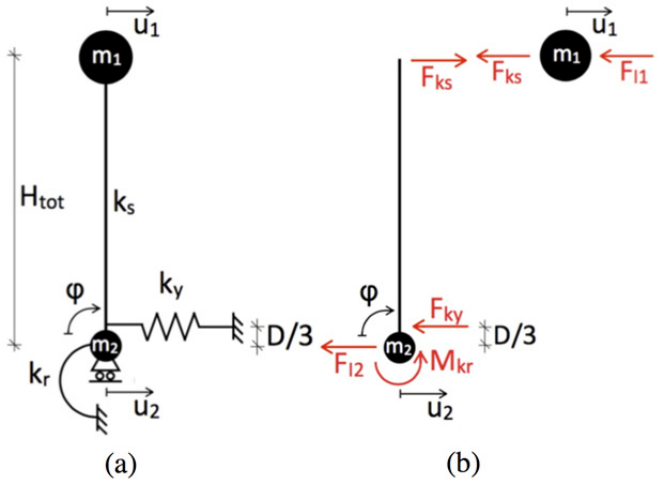

Figure 2. Simplified spring model (a) and free body diagram (b).

The resulting forces (F_{ks} and F_{ky}) and moment (M_{kr}) in the springs can be formulated as a function of spring's stiffness (k_s, k_y and k_r) and their displacement (u_1 and u_2) and rotation (φ) respectively:

$$F_{ks} = k_s \cdot (u_1 - u_2 - \varphi \cdot H_{tot}) \quad (1)$$

$$F_{ky} = k_y \cdot \left(u_2 + \frac{d}{3} \cdot \varphi\right) \quad (2)$$

$$M_{kr} = k_r \cdot \varphi \quad (3)$$

The inertia forces acting on the masses are:

$$F_{I1} = m_1 \cdot \ddot{u}_1 \quad (4)$$

$$F_{I2} = m_2 \cdot \ddot{u}_2 \quad (5)$$

Using equations (1) to (5), an equilibrium equation can be formulated for every degree of freedom (u_1, u_2 and φ):

$$m_1 \cdot \ddot{u}_1 + k_s \cdot (u_1 - u_2 - \varphi \cdot H_{tot}) = 0 \quad (6)$$

$$m_2 \cdot \ddot{u}_2 + k_Y \cdot \left(u_2 + \frac{d}{3} \cdot \varphi\right) - k_s \cdot (u_1 - u_2 - \varphi \cdot H_{tot}) = 0 \quad (7)$$

$$k_r \cdot \varphi + \frac{d}{3} \cdot k_Y \cdot \left(u_2 + \frac{d}{3} \cdot \varphi\right) - H_{tot} \cdot k_s \cdot (u_1 - u_2 - \varphi \cdot H_{tot}) = 0 \quad (8)$$

Since mass m_2 is modeled as a point mass, its rotational inertia can be neglected. After this assumption only two independent degrees of freedom (u_1 & u_2) predominate the motion. After some mathematical operations the equation of motion is represented in the following matrix form:

$$\begin{bmatrix} m_1 & 0 \\ 0 & m_2 \end{bmatrix} \cdot \begin{pmatrix} \ddot{u}_1 \\ \ddot{u}_2 \end{pmatrix} + \begin{bmatrix} k_{11} & k_{21} \\ k_{12} & k_{22} \end{bmatrix} \cdot \begin{pmatrix} u_1 \\ u_2 \end{pmatrix} = \begin{pmatrix} 0 \\ 0 \end{pmatrix} \quad (9)$$

Where

$$k_{11} = k_s - \frac{H_{tot}^2 \cdot k_s^2}{k_r + H_{tot}^2 \cdot k_s + \frac{d^2}{9} \cdot k_y} \quad (10)$$

$$k_{12} = k_{21} = -k_s + \frac{H_{tot}^2 \cdot k_s^2 + H_{tot} \cdot \frac{d}{3} \cdot k_s \cdot k_y}{k_r + H_{tot}^2 \cdot k_s + \frac{d^2}{9} \cdot k_y} \quad (11)$$

$$k_{22} = k_y + k_s - \frac{H_{tot} \cdot k_s + \frac{d}{3} \cdot k_y}{k_r + H_{tot}^2 \cdot k_s + \frac{d^2}{9} \cdot k_y} \cdot \left(\frac{d}{3} \cdot k_y + H_{tot} \cdot k_s\right) \quad (12)$$

The natural frequencies of the 2-DOF system are directly calculated from the mass and stiffness matrix by use of modal analysis.

2.1.3 *Spring stiffness and soil parameters*

The springs of the structural model are linear elastic. Therefore their applicability is limited to cases in which the stress - strain behavior can be represented adequately by a linear relation. The superstructure stiffness is given from the column geometry (I_{column}) and the Young's modulus of aluminum (E_{al}):

$$k_s = \frac{3 \cdot E_{al} \cdot I_{column}}{H_{tot}^3} \quad (13)$$

The stiffness of the springs, which represent the soil-structure interaction in the simplified system, are calculated by following the procedure for embedded foundations proposed by Gazetas (1991).

The first set of input parameters is defined by the foundation geometry: foundation width B, foundation shape (round or square) and embedment depth D. The second sets of input parameters are elastic soil parameters: Poisson's ratio ν and shear modulus G. These two sets of parameters allow to calculate an equivalent static stiffness of the springs. The equations from Gazetas (1991) would also allow to estimate the stiffness of harmonic vibrating foundations using a dynamic factor. However, as in these set of experiments no harmonic vibration and only small deformation are expected, static stiffness values were used. The structure is excited by an impulse excitation and after this first stimulation is free to vibrate until the energy is completely dissipated.

For square shaped foundations the equation for the horizontal spring stiffness is reduced to:

$$k_y = \frac{2 \cdot G \cdot L}{2 - \nu} \cdot 4.5 \cdot \left(1 + 0.15 \cdot \left(\frac{D}{B}\right)^{0.5}\right) \cdot \left(1 + 0.52 \cdot \left(\frac{2 \cdot D}{B}\right)^{0.8}\right) \quad (14)$$

The stiffness of the rotational spring reduces to:

$$k_r = \frac{3 \cdot G}{1 - \nu} \cdot \left(\frac{4 \cdot B}{3}\right)^{0.75} \cdot \left(1 + 0.92 \cdot \left(\frac{D}{B}\right)^{0.6} \cdot \left(1.5 + \left(\frac{D}{B}\right)^{1.3}\right)\right) \quad (15)$$

While all geometric parameters of the model are well known, it is more challenging to describe the elastic soil parameters ν (Poisson ratio) and G (shear modulus). For sand a Poisson ratio of 0.3 was used (Hamilton 1979). The Equations 14 & 15 assume a homogenous soil with constant shear modulus G. This assumption does not hold in our experiment since the confining stresses increase with depth and therefore the shear modulus also increases with depth (G (z)). However, in order to keep the model simple and to be able to use the presented equations, a typical

value of the shear modulus is assessed using the following assumptions:

- A representative shear modulus is chosen G = G(z = const.) = const
- Shear strains are assumed to be very small and therefore G = G_{max}.

Since this study focused on the behavior of shallow foundation, a representative shear modulus would be one near the surface approximately between one and four meters below the ground surface.

Several experiments like the one conducted by Murillo et al. (2009) were also conducted on the Perth sand with the geotechnical drum centrifuge at ETH-Zurich (Martakis 2016). The goal of these experiments was to estimate the shear wave velocity V_s of the soil near the surface and consequently the shear modulus for small strains G_{max}. To achieve that the tests were based on the Spectral Analysis of Surface Waves (SASW) method. The results of the physical modeling analysis conducted by Martakis (2016) suggested that the maximal shear modulus G_{max} near the surface can be approximated by 30 MPa. This value is characteristic for a medium dense sand with a dry density of ρ_d = 1.7 t/m^3 at low confining stresses.

2.2 *Physical modeling experiment*

Physical modeling experiments were conducted with the purpose of simulating the soil structure interaction of a free vibrating system after an impulse excitation in an enhanced g-level environment. All the experiments were conducted at 60g and the geometrical dimensions are in model scale. The goal of the experiments were:

- to find the period lengthening ratio between the natural frequency of the soil-structure system and the fixed base
- and to verify the performance of the analytical model compared with physical experiment.

2.2.1 *Experimental setup*

The soil layer is filled in the soil container by air pluviation. The soil is released from a height of 40 cm out of a cone equipped with a sieve. The height of fall is kept constant. The density of the soil is controlled by the diameter of the opening of the cone. A smaller diameter should provide a denser soil, while a larger diameter should provide a looser soil. With this method it was possible to reach a dry density ρ_d of 1.7 t/m^3. In total two accelerometers are placed on the metallic surface of the models. One is installed at top of the structure and the other one on the foundation.

The positions of the accelerometers are shown in Figure 3. The accelerometers measure acceleration in the horizontal direction. Details on the accelerometers can be found in Chikatamarla et al. (2006). The impulse excitation is produced by the impact of a light ball. The ball is accelerated by the centripetal forces inside the centrifuge (Figure 3) and hits the head of the structures on a trajectory parallel to the surface of the soil.

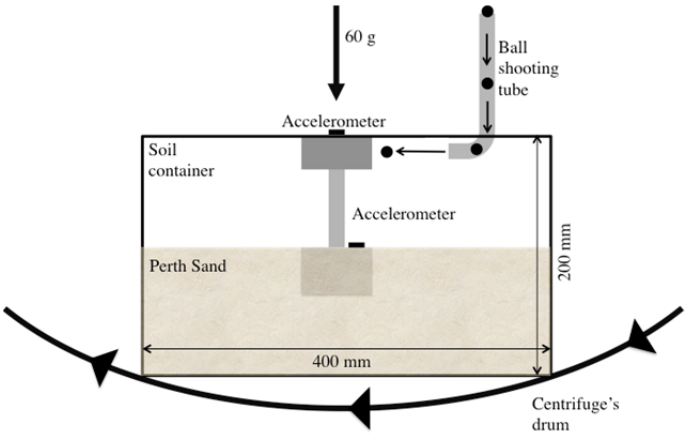

Figure 3. Schematic representation of the experimental setup.

3 RESULTS

3.1 *Analytical results*

In order to validate the analytical solution for the simplified spring model suggested in the previous sections, the period lengthening ratio obtained with this simplified spring model is compared to the solution of period lengthening ratio given in equation (16) and proposed by Chen et al. (2013).

$$\frac{f_1}{f} = \sqrt{1 + \frac{k_s}{k_y} + \frac{k_s \cdot H_{tot}^2}{k_r}} \tag{16}$$

Figure 4 shows that the simplified model has a correlation with the empirical PLR-formula recommended by Chen et al. (2013). That means that the simplified spring model is reliable for capturing the natural frequencies of the various soil-structure setups.

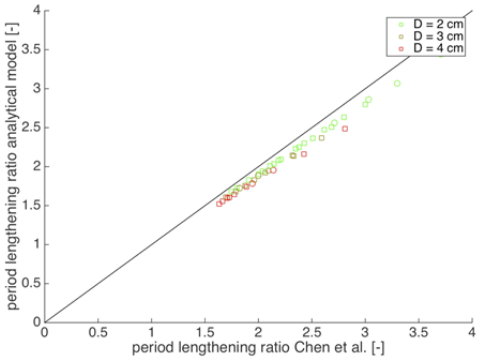

Figure 4. Comparison between the calculated and the empirical PLR suggested by Chen et al. (2013).

3.2 *Physical modeling vs. analytical results*

Figure 5a illustrates the typical time history of the original signal, the filtered signal and the signal after downsampling. The ball hits the head of the superstructure and from this moment the structure starts to vibrate freely and the foundation starts to rock.

It is clearly visible, that the original data includes both high frequency and low frequency content. Since the interesting part of the signal has a medium frequency content, the noisy part of the signal is removed by use of a bandpass filter. Frequencies below 150 Hz and above 800 Hz (model scale) were filtered out. Figure 5b represents the Fourier spectra corresponding to the time history diagram shown in Figure 5a.

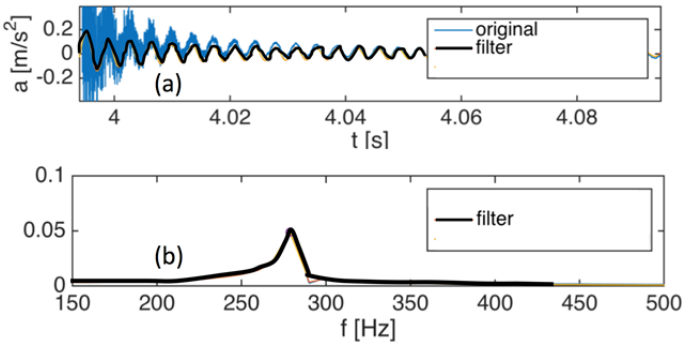

Figure 5. Time history of the free vibrating structure (a) and its corresponding Fourier spectra (b).

Figure 6 shows that for a G-modulus of 30 MPa, the PLR ratio of all evaluated models is more or less the same for the experimental and the analytical solution (correlation of 0.98).

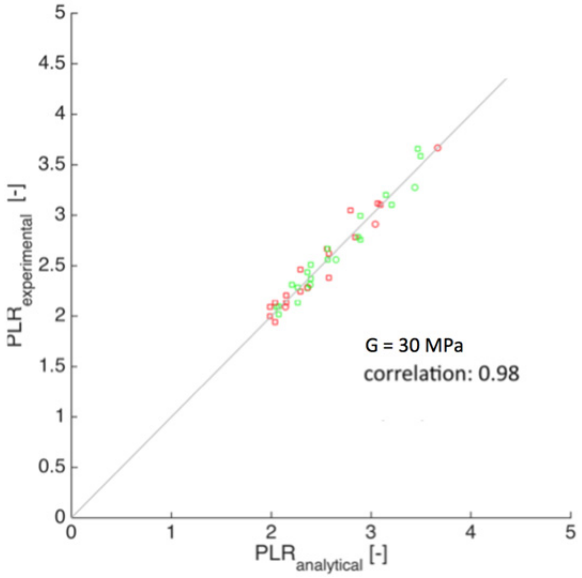

Figure 6.Experimental vs. analytical results of the PLR

3.3 *PLR as function of the geometry*

As shown in Figure 7 it can be seen that the PLR is strongly dependent on the H/B ratio. If the width B of foundation stays constant and the height H of the superstructure increases, the PLR decreases almost linearly. On the contrary if the height H of the superstructure stays constant and the width B increases, the PLR increases as well. It means that an increment of the width B of the foundation has a bigger impact on the period elongation of the soil-structure system.

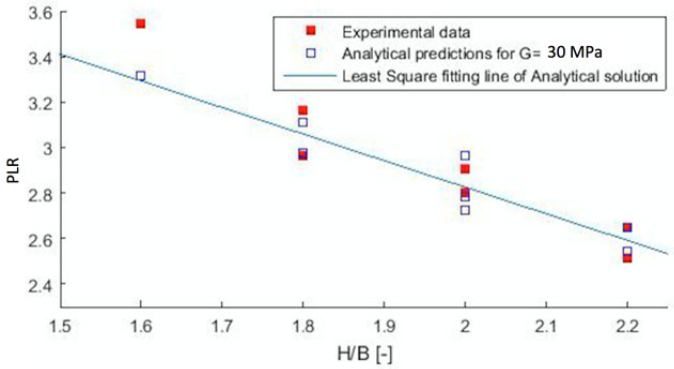

Figure 7. PLR as a function of the H/B ratio.

4 CONCLUSIONS

This study demonstrated that the period lengthening ratio (PLR) depends on the superstructure, the foundation and the soil. The parameters of this problem and their influence on the PLR are summarized in Table 2.

Table 2. Parameter effect on PLR.

Parameter	Period elongation
G ↑	PLR ↓
H ↑	PLR ↓
B ↑	PLR ↑
D↑	PLR ↓

The period elongation and the soil structure interaction cannot be neglected during the design of embedded structures. Figure 8 illustrates that in the Swiss code design norm, the dynamic acceleration response of a fixed base structure (S_e / a_{gd} =1.9) is much smaller compared to the one that considers an interaction between the superstructure and the soil (S_e / a_{gd} =2.7). S_e is the response spectra of the horizontal ground acceleration and a_{gd} is the dimensioning value of horizontal ground acceleration, which corresponds to the maximum horizontal ground acceleration for a reference return period of 475 years (Swiss code, S.I.A 261 2003). That means that the assumption of a fixed base structure underestimates the acceleration response of the construction during seismic excitation.

Within the centrifuge experiments, a large number of structures with rather short fixed-base periods (0.06 s < $T_{1,prototype}$ < 0.23 s) has been analyzed. It would also be interesting to quantify the PLR of structures with higher natural period.

Commonly especially tall buildings are often designed close to the maximal allowed period in terms of serviceability under wind loads and therefore, it is desirable to have a good estimate of the period elongation due to SSI. Physical modeling experiments at higher g – level could simulate taller embedded construction with larger period $T_{1,prototype}$.

Within the context of conducted experiments, light drop weights were adopted, resulting in response that mostly lied in the elastic region. Further tests should be conducted with heavier balls so that the inelastic response of the system can also be analyzed.

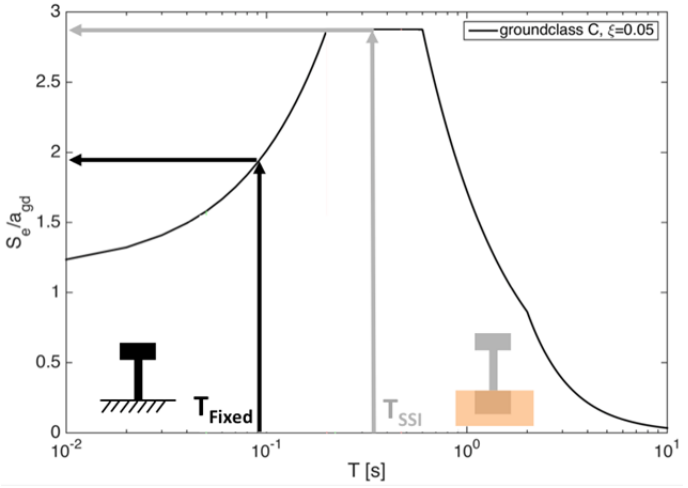

Figure 8. The effect of the period elongation on the elastic response spectra.

5 ACKNOWLODGEMENT

This research was supported by the master students M. Lee, C. Buss, D.T. Tran and L. Lampach and the postdoctoral research associate V. Dertimanis. Their help and contribution during the experiments and the evaluation of the results was crucial. We also wish to express our sincere gratitude to the centrifuge technician M. Iten for assisting us during the laboratory exepriments.

6 REFERENCES

Anastasopoulos, I., Loli, M., Georgarakos, T., & Drosos, V. 2013. Shaking Table Testing of Rocking—Isolated Bridge Pier on Sand. *Journal of Earthquake Engineering 17*(1): 1-32.

Chen, Z., Trombetta, N. W., Hutchinson, T. C., Mason, H. B., Bray, J. D., & Kutter, B. L. 2013. Seismic System Identification Using Centrifuge-based Soil-Structure Interaction Test Data. *Journal of Earthquake Engineering*, *17*(4): 469-496.

Chikatamarla, R., Laue, J., & Springman, S. M. 2006. Centrifuge scaling laws for guided free fall events including rockfalls. *International Journal of Physical Modelling in Geotechnics*, *6*(2): 15-26.

Gazetas, G. 1991. Formulas and charts for impedances of surface and embedded foundations. *Journal of Geotechnical Engineering*, *117*(9): 1363-1381.

Hamilton, E. L. 1979. Vp/Vs and Poisson's ratios in marine sediments and rocks. *The Journal of the Acoustical Society of America*, *66*(4): 1093-1101.

Kausel, E., Whitman, R. V., Morray, J. P., & Elsabee, F. 1978. The spring method for embedded foundations. *Nuclear Engineering and Design*, *48*(2): 377-392.

Martakis, P. 2016. *A centrifuge – experimental study in the soil and structure interaction effect on a SDOF system* (Master thesis, Eidgenössische Technische Hochschule ETH Zürich).

Murillo, C. A., Thorel, L., & Caicedo, B. 2009. Spectral analysis of surface waves method to assess shear wave velocity within centrifuge models. *Journal of Applied Geophysics*, *68*(2): 135-145.

Nazarian, S., & Stokoe, K. H. 1984. In situ shear wave velocities from spectral analysis of surface waves. In *Proceedings of the 8th world conference on earthquake engineering* 3: 31-38).

Peñuela, W. F. M. 2013. *River dyke failure modeling under transient water conditions* (Doctoral dissertation, Diss., Eidgenössische Technische Hochschule ETH Zürich, Nr. 21580, 2013).

Sieffert, J.G. & Cevaer, F. 1995. *Handbook of Impedance Functions*. Nantes: Ouest Editions.

Springman, S., Laue, J., Boyle, R., White, J., & Zweidler, A. 2001. The ETH Zurich geotechnical drum centrifuge. *International Journal of Physical Modelling in Geotechnics 1*(1): 59-70.

Swiss Code, S. I. A. 261, 2003. Actions on Structures. *Swiss Society of engineers and architects*.

.